

## PAPER

[View Article Online](#)  
[View Journal](#) | [View Issue](#)Cite this: *RSC Mechanochem.*, 2024, 1, 235Grinding and the anisotropic environment:  
influences on the diastereoselective formation of  
Group 15 allyl complexes†

Lauren E. Wenger and Timothy P. Hanusa \*

The heavy Group 15 allyls  $[EA'_3]$  ( $E = \text{As, Sb, Bi}$ ;  $[A'] = [1,3-(\text{SiMe}_3)_2\text{C}_3\text{H}_3]^-$ ) can be prepared either in solution or mechanochemically, and exist in two diastereomeric forms of  $C_1$  and  $C_3$  symmetry. For  $E = \text{As}$  and  $\text{Sb}$ , their ratio varies with the method of preparation: the  $C_1$  diastereomer is the major form by both methods, but the mechanochemical route increases the  $C_1 : C_3$  ratio compared to synthesis in hexanes solution. The difference in selectivity has previously been identified as a consequence of the layered crystal lattices of the  $\text{EX}_3$  reagents, which provide a templating effect through an anisotropic grinding environment. How this selectivity changes with other typical mechanochemical variables is explored here, including the use of different reagents and LAG solvents, pre-grinding the reagents, the use of different milling media (stainless steel, Teflon, etc.) and apparatus (mixer mill, planetary mill), and the number and size of balls. The extent to which the anisotropic environment is either maintained or modified during synthesis (especially by LAG and the choice of metal reagent) affects the diastereomeric ratio.

Received 4th January 2024

Accepted 21st March 2024

DOI: 10.1039/d4mr00001c

[rsc.li/RSCMechanochem](https://rsc.li/RSCMechanochem)

## Introduction

Despite its longstanding history,<sup>1</sup> mechanochemistry as a systematically explored approach to synthesis and reactivity has experienced enormous development in the past quarter century. To call its recent growth “explosive” would be a serious understatement (a recent review noted that more than 500 papers concerned with mechanochemical phenomena were published each year during the past decade).<sup>2</sup> As the use of mechanochemistry for organic, inorganic, and organometallic synthesis grows, it becomes increasingly important to understand the reaction mechanism(s) involved and how various experimental parameters affect outcomes.<sup>3</sup> Some of these variables have direct counterparts in solution chemistry, such as reaction times, reagent stoichiometry, and temperature. Others are known to be important in mechanochemical synthesis, even if their effects are not always well understood, such as the mill or mixer type, ball and jar material, the size and number of ball bearings, and the use of additives (*e.g.*, liquid-assisted grinding (LAG), dry grinding agents).<sup>4</sup> A less common and more poorly understood variable, and one that has no direct solution analog, is the crystal structure of solid reagents, particularly those with anisotropic (*e.g.*, layered) lattices.<sup>5</sup>

We have previously explored the formation of the heavy Group 15 allyls  $[EA'_3]$  ( $E = \text{As, Sb, Bi}$ ;  $[A'] = [1,3-(\text{SiMe}_3)_2\text{C}_3\text{H}_3]^-$ ), which can be prepared either in solution or mechanochemically from  $\text{EX}_3$  and  $\text{K}[A']$  (for As, Sb) or  $[\text{AlA}_3]$  (for Bi).<sup>5</sup> The  $[EA'_3]$  complexes are generated in two diastereomeric forms, one of  $C_1$  symmetry and the other of  $C_3$  symmetry (Fig. 1), and for  $E = \text{As}$  and  $\text{Sb}$  their ratio varies with the method of preparation (for  $E = \text{Bi}$ , the ratio is essentially the same for both reaction environments). The halide metathetical synthetic approach is not successful for all combinations of reagents. For example,  $\text{AsI}_3$  and  $\text{K}[A']$  in THF solution, or  $\text{BiCl}_3$  and  $\text{K}[A']$  in the solid state, initiate a redox reaction leading to allyl coupling and the formation of 1,3,4,6-tetrakis(trimethylsilyl)hexa-1,5-diene ( $\{A'\}_2$ ) as the major product.

The  $C_1$  diastereomer is the major form by both methods for both As and Sb, but the mechanochemical route increases the

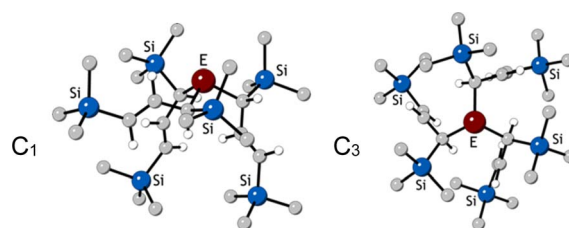


Fig. 1 Diastereomeric forms of  $[EA'_3]$ . The  $C_1$  form is crystallographically characterized for  $E = \text{As, Sb}$ ; the  $C_3$  forms have been identified from NMR spectroscopy and their structures studied computationally.<sup>5</sup>

Department of Chemistry, Vanderbilt University, Nashville, Tennessee, 37235, USA.

E-mail: [t.hanusa@vanderbilt.edu](mailto:t.hanusa@vanderbilt.edu)† Electronic supplementary information (ESI) available. See DOI: <https://doi.org/10.1039/d4mr00001c>

relative amount of  $C_1$  by 3.3 times for As and 1.5 times for Sb, compared to preparation in hexanes solution. This difference in selectivity has been attributed to the layered crystal lattice of each metal precursor (Fig. 2 and Table S1†).<sup>5</sup> Density functional theory (DFT) calculations have been used to demonstrate that when arsenic is embedded in an  $AsI_3$  lattice (Fig. 2b), the first allyl to bind to As will preferentially be aligned parallel to the lattice planes of  $AsI_3$ , thereby avoiding excessive steric interaction (Fig. 3a). The second allyl will then most easily bind perpendicularly to the first; calculations indicate that the lower energy isomer of the intermediate  $[AsA'_2I]$  contains allyls of opposite handedness, *i.e.*  $[As(R-A')(S-A')I]$  is lower in energy than  $[As(R-A')_2I]$  by 11.5 kJ mol<sup>-1</sup>.<sup>5</sup> Setting the stereochemistry in this step leads to a preference for the  $C_1$  form in the solid state. In contrast, for a  $[AsI_2A']$  unit in solution, the  $C_3$  backbone of the allyl is arranged roughly perpendicularly to a line connecting the iodides (*i.e.*, 90° from the solid-state orientation). There is not a strong stereochemical preference for the subsequent orientations of the other allyl ligands, raising the probability of generating the  $C_3$  form in solution (Fig. 3b). The weaker preference for the  $C_1$  form in  $[SbA'_3]$  is likely the result of the zig-zag layers of  $SbCl_3$  enforcing the stereochemically directed assembly less strictly than does the planar geometry of  $AsI_3$ .

The original report of  $[EA'_3]$  synthesis found that the  $C_1 : C_3$  ratio of the mechanochemically prepared compounds was relatively constant over a range of grinding times in a planetary mill with stainless steel grinding balls (5 min to 2 h), although at very short reaction times (30 s), the  $C_1 : C_3$  ratio of  $[AsA'_3]$  was somewhat higher, suggesting that  $C_1$  is the more rapidly formed diastereomer.<sup>5</sup> We were interested in determining whether other mechanochemical reaction variables, including the mill type, jar and ball material, size of balls, operation of liquid assisted grinding (LAG),<sup>6</sup> or changes in metal precursor (two different halides are now used for both As and Sb), could lead to alterations in the diastereomer selectivity.

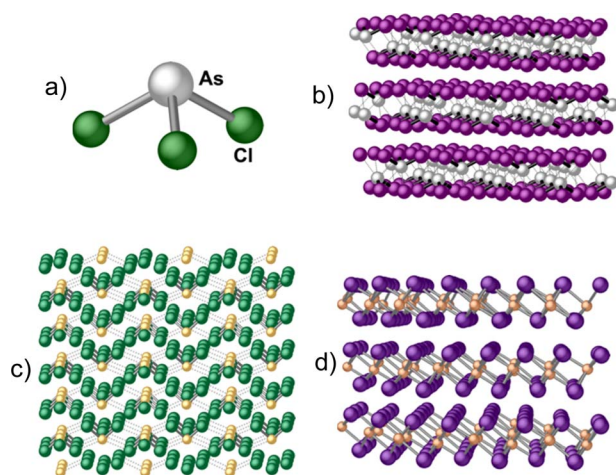


Fig. 2 Structures of  $MX_3$  ( $M = As, Sb$ ;  $X = Cl, I$ ): (a)  $AsCl_3$  (liquid at room temperature); (b) lattice of  $AsI_3$ ; (c) lattice of  $SbCl_3$ ; (d) lattice of  $SbI_3$ . See Table S1† for details of the structures.

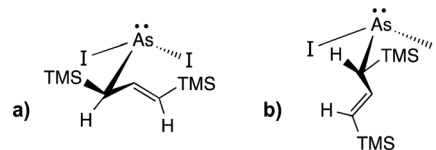


Fig. 3 (a) Preferred conformation of an  $[AsA'I_2]$  unit when the  $[AsI_2]$  fragment is part of the  $AsI_3$  lattice; (b) Lowest energy conformation of an  $[AsA'I_2]$  unit in solution. TMS = trimethylsilyl.

The mechanochemical formation of diastereomeric  $[EA'_3]$  complexes serves as a valuable model system to investigate the potential amplification or suppression of the effects of an anisotropic reaction environment. Furthermore, it sheds light on how manipulating this environment might affect the balance between halide metathesis and redox behavior.

## Experimental

In accordance with the literature procedure,<sup>5</sup>  $[AsA'_3]$  was prepared mechanochemically from  $AsI_3$  or  $AsCl_3$  and 3 equiv. of  $K[A']$  under various milling conditions.  $[SbA'_3]$  was prepared analogously from  $SbCl_3$  or  $SbI_3$  and 3 equiv. of  $K[A']$ . Additional experimental details are provided in the ESI.† This section highlights the relevant changes from the literature procedure, which fall into four categories: LAG, pre-grinding, changes in metal precursor, and mechanochemical equipment variables.

For all conditions, each experiment was performed in at least duplicate and often triplicate. For each reaction,  $^1H$  NMR data was used to determine the  $C_1 : C_3$  ratio, yield of  $[EA'_3]$ , and the  $[EA'_3] : \{A'\}_2$  ratio.

### LAG

In these reactions, 1 to 60 equiv. of the LAG solvent was added to dry reagents before grinding. LAG solvents included hexanes, hexamethyldisiloxane (HMDSO), and tetrahydrofuran (THF) for the arsenic system, and hexanes for the antimony system (see Tables S4, S5 and S10†).

### Pre-grinding

To determine the effect of possible lattice degradation, the metal halide precursor was ground alone with ball bearings for a varied amount of time (pre-grinding time) before adding  $K[A']$ , followed by grinding again with a fixed reaction time. This was done using both the planetary mill and mixer mill; these experiments used stainless steel milling equipment (see Tables S6 and S11†).

### Metal precursor

Solution (toluene only) and mechanochemical reactions (mixer mill only) of  $AsCl_3$  (a liquid) were compared to reactions employing  $AsI_3$  (a solid). Mechanochemical reactions of  $SbI_3$  were compared to those with  $SbCl_3$  (both solids), including pre-grinding experiments, and changing the mill type and jar and ball material used.



## Mechanochemical equipment variables

The original report described experiments that varied only reaction time.<sup>5</sup> This investigation probed the effects of mill type (mixer or planetary), jar and ball material (stainless steel, Teflon, zirconia), and ball size (4.8 mm vs. 9.5 mm stainless steel balls) at multiple reaction times (see Tables S3 and S9†).

## Decomposition studies

The reaction between  $\text{AsI}_3$  and  $\text{K}[\text{A}']$  is rapid, with up to quantitative yield observed in 5 min and the yield generally decreasing at longer reaction times. After the reaction is complete, the remaining time (up to 55 min) involves milling of the generated  $[\text{AsA}'_3]$  and other products (potassium iodide,  $\{\text{A}'\}_2$ , elemental As), leading to decomposition of  $[\text{AsA}'_3]$  to form more  $\{\text{A}'\}_2$ . Therefore, decomposition studies were performed to better understand how reaction time affects the production of  $[\text{AsA}'_3]$  and  $\{\text{A}'\}_2$ . Specifically,  $[\text{AsA}'_3]$  was milled alone or with 3 equiv. of potassium iodide in the mixer mill for 30–60 min with small or large stainless steel ball bearings (see Table S7†). For comparison, prepared  $[\text{AsA}'_3]$  was dissolved in toluene- $d_8$  in an NMR tube and heated in an oil bath at 90 °C for 7.5 h, and the outcome monitored with  $^1\text{H}$  NMR.

## Results

### Variable 1: use of LAG

Under LAG conditions using non-coordinating hexanes or HMDSO, the  $\text{C}_1:\text{C}_3$  ratio of  $[\text{AsA}'_3]$  decreased with increasing amounts of solvent. The addition of a small volume of hexanes modifies the  $\text{C}_1:\text{C}_3$  ratio quickly: mechanochemical enhancement compared to solution is cut in half by *ca.* 3.5 equiv. of hexanes ( $\eta = 0.41$ )<sup>6</sup> (Fig. 4). Arsenic triiodide has low, but detectable solubility in hexanes;<sup>7</sup> in contrast it has no measurable solubility in HMDSO. Nevertheless, HMDSO displays similar effects on the  $\text{C}_1:\text{C}_3$  ratio (Fig. 4); 3 equiv. reduces the  $\text{C}_1:\text{C}_3$  excess by half ( $\eta = 0.56$ ). From dry grinding to solution conditions, the changes in  $\text{C}_1:\text{C}_3$  ratios in the LAG reactions follow a simple power curve.

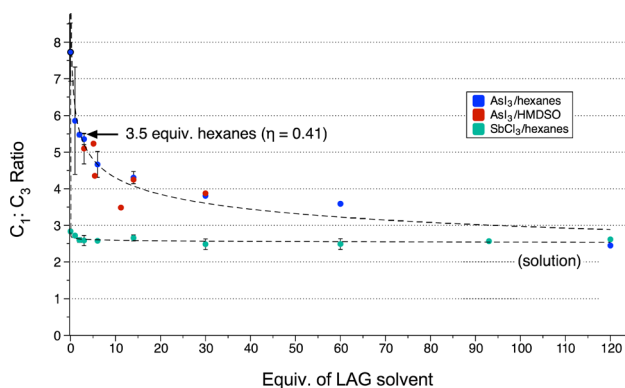


Fig. 4 LAG effects on diastereomer formation in  $[\text{AsA}'_3]$  with hexanes and HMDSO, and in  $[\text{SbA}'_3]$  with hexanes. The top dotted line is the power law fit to the  $\text{AsI}_3/\text{hexanes}$  data ( $y = 6.23x^{-0.16}$ ;  $R^2 = 0.94$ ); the bottom line fits the  $\text{SbCl}_3$  data ( $y = 2.64x^{-0.0086}$ ;  $R^2 = 0.67$ ).

LAG with THF prevents formation of  $[\text{AsA}'_3]$ . In the presence of THF,  $\text{K}[\text{A}']$  can reversibly form the solvent adduct  $\{\text{K}[\text{A}'](\text{thf})_{3/2}\}$ .<sup>8</sup> This might be the reason that the use of 4.5 equiv. ( $\eta = 0.33$ ) of THF (and 3  $\text{K}[\text{A}']$ ) completely blocks product formation, yielding only recovered starting material. Using more THF (10 or 13 equiv.,  $\eta = 0.81$  and  $0.95$ , respectively), affords  $\{\text{A}'\}_2$  as the major product ( $\{\text{A}'\}_2: [\text{AsA}'_3] = 2.4, 2.8$ ) with low  $\text{C}_1:\text{C}_3$  ratios (3.5, 3.3), close to that found in the preparation from hexanes solution (see Table S5†). As noted above, the solution-based reaction in THF produces  $\{\text{A}'\}_2$  as the major identified product.<sup>5</sup> Once prepared, however,  $[\text{AsA}'_3]$  is stable in THF- $d_8$  solution ( $^1\text{H}$  NMR), indicating that the difficulty with THF is only in the formation of  $[\text{AsA}'_3]$ , not with its subsequent reactivity.

For  $[\text{SbA}'_3]$ , LAG was performed for reactions of  $\text{SbCl}_3$  and 3 equiv. of  $\text{K}[\text{A}']$  with hexanes. As with the arsenic system, the  $\text{C}_1:\text{C}_3$  ratio decreases with increasing solvent, but the trend is less pronounced, in part due to the lower magnitude of change between dry grinding and solution conditions (Fig. 4). Here, the reduction in the preference for  $\text{C}_1:\text{C}_3$  by 50% requires the addition of 17 equiv. of hexanes ( $\eta = 2.4$ ), which is firmly in the “slurry” region of the LAG range.<sup>6</sup>

For both  $[\text{AsA}'_3]$  and  $[\text{SbA}'_3]$ , trends in the yield of  $[\text{EA}'_3]$  or  $[\text{EA}'_3]:\{\text{A}'\}_2$  ratio do not show clear correlations with increasing addition of solvent, so it remains uncertain what role the solvent plays in the competing reactions of metathesis and redox (see Fig. S6, S7, S15 and S16†).

### Variable 2: pre-grinding

Pre-grinding of  $\text{AsI}_3$  was performed in a planetary mill at 600 rpm (maximum speed) for 1 to 45 min or in a mixer mill at 30 Hz (maximum speed) or 10 Hz for 1 to 30 min. Powder X-ray diffraction of  $\text{AsI}_3$  itself ground for 45 min in a planetary mill shows only  $\text{AsI}_3$  and no reduced arsenic or iodine species (Fig. S25†). Using the pre-ground  $\text{AsI}_3$  in the synthesis of  $[\text{AsA}'_3]$  does reveal a decrease in the  $\text{C}_1:\text{C}_3$  ratio, but only when using the planetary mill. The  $\text{C}_1:\text{C}_3$  ratio decreases *ca.* 27% over 45 min (linear equivalent =  $-0.053 \text{ min}^{-1}$ ). However, the  $\text{C}_1:\text{C}_3$  ratio does not approach that from a solution reaction

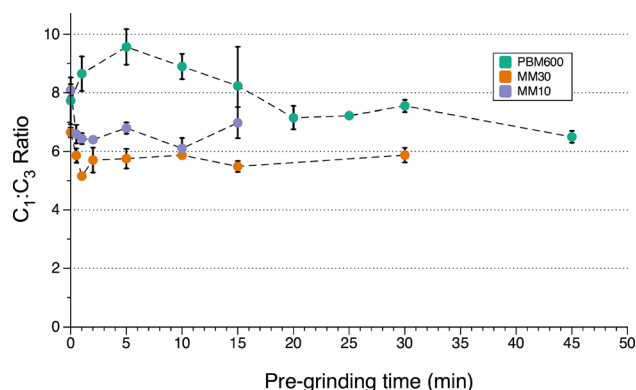


Fig. 5 Effect of pre-grinding  $\text{AsI}_3$  on diastereomer formation. PBM600 = planetary mill, 600 rpm; MM30 = mixer mill at 30 Hz; MM10 = mixer mill at 10 Hz.



during that time (Fig. 5). The yield and  $[\text{AsA}'_3]:\{\text{A}'\}_2$  ratio also trended downward with increased pre-grinding time (see Fig. S8 and S9†).

With a mixer mill, in contrast, the  $\text{C}_1:\text{C}_3$  ratio was nearly constant at 30 Hz over all pre-grinding time points (Fig. 5). Visual inspection showed no significant change in the appearance of  $\text{AsI}_3$  with pre-grinding time. After 1 min, the solid was finely ground and appeared similar to that ground for 30 min (see Fig. S22†). The higher energy collisions from the larger ball bearings and faster speed in the mixer mill likely erased any trend in the  $\text{C}_1:\text{C}_3$  ratio of  $[\text{AsA}'_3]$  by reaching a small particle size more quickly than in the planetary mill. In order to determine whether an effect was obvious with lowered energy input, the energy of both pre-grinding and the reaction were reduced by pre-grinding at 10 Hz and performing the reaction for 5 min instead of 10 min. Although there is a visual change in particle size from the shortest to longer pre-grinds (see Fig. S19–S21†), there is again no obvious trend in the  $\text{C}_1:\text{C}_3$  ratio (Fig. 5).

Pre-grinding of  $\text{SbCl}_3$  was performed at 300 rpm in a planetary mill for 1 to 60 min or in the mixer mill at 20 Hz for 1 to 45 min. (The decreased frequencies in the mills match those of the optimized reaction conditions for  $[\text{SbA}'_3]$ .)  $\text{SbI}_3$  was pre-ground at 300 rpm in the planetary mill for 1 to 45 min.

In the planetary mill, extended pre-grinding led to a slight decrease in  $\text{C}_1:\text{C}_3$  for both  $\text{SbI}_3$  and  $\text{SbCl}_3$  (Fig. 6). The decrease was less than that of  $\text{AsI}_3$  under the same conditions (*ca.* 7% decrease for  $\text{SbI}_3$  after 45 min and a 10% decrease for  $\text{SbCl}_3$  in 60 min). Similar to the case with  $\text{AsI}_3$ , when  $\text{SbCl}_3$  was pre-ground in the mixer mill there was no significant decrease in the  $\text{C}_1:\text{C}_3$  ratio over time. Instead, mixer mill pre-grinding led to a significant decrease in both yield (–36%) and the  $[\text{SbA}'_3]:\{\text{A}'\}_2$  ratio with increased pre-grinding time (see Fig. S17 and S18†). Pre-grinding in the planetary mill led to small increases in these values as pre-grinding time increased (*e.g.*, the yield rose from 31% (no pre-grinding) to 42% (pre-grinding  $\text{SbCl}_3$  for 60 min)). This suggests that the type of mill impacts the competition between metathesis and redox pathways.

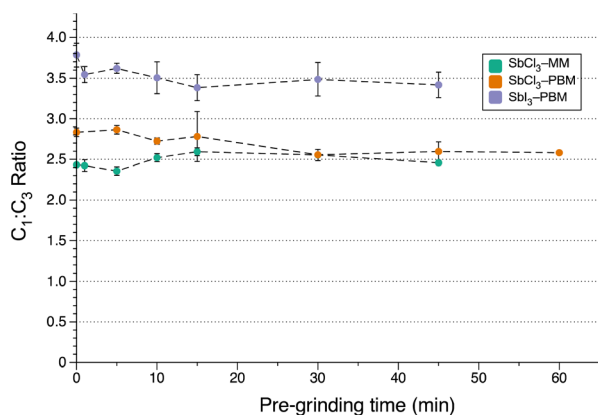


Fig. 6 Effect of pre-grinding  $\text{SbX}_3$  on diastereomer formation.  $\text{SbCl}_3\text{-MM}$  =  $\text{SbCl}_3$  in mixer mill;  $\text{SbCl}_3\text{-PBM}$  =  $\text{SbCl}_3$  in planetary mill;  $\text{SbI}_3\text{-PBM}$  =  $\text{SbI}_3$  in planetary mill.

Although not as extensively studied as the pre-grinding experiments, several trials were conducted to explore the effect of variable frequency on the formation of  $[\text{SbA}'_3]$ . Grinding  $\text{K}[\text{A}']$  and  $\text{SbCl}_3$  at 20 Hz in a mixer mill for 10 min produced the highest yield ( $70 \pm 10\%$ ), with a  $\text{C}_1:\text{C}_3$  ratio of  $2.53(\pm 0.05)$  and a  $[\text{SbA}'_3]:\{\text{A}'\}_2$  ratio of  $6(\pm 3)$ . Raising the frequency to 30 Hz for the same length of time marginally improved the  $\text{C}_1:\text{C}_3$  ratio (2.66), but the yield dropped to 49%, and the  $[\text{SbA}'_3]:\{\text{A}'\}_2$  ratio decreased to 3.6. At 15 Hz, not only was the  $\text{C}_1:\text{C}_3$  ratio lowered to 2.31, but also the reaction was incomplete, as unreacted  $\text{K}[\text{A}']$  could be detected among the reaction products ( $^1\text{H}$  NMR). It seems that although there is a modest boost (5%) to the  $\text{C}_1:\text{C}_3$  ratio on going from 20 to 30 Hz, there is actually only a narrow window of usable frequencies for the optimum yield and maximum  $[\text{SbA}'_3]:\{\text{A}'\}_2$  ratio.

### Variable 3: elemental precursor

Whereas the original report used only  $\text{AsI}_3$  and  $\text{SbCl}_3$  as precursors, the present study used two arsenic precursors and two antimony precursors. The use of a layered solid reagent directs the increase in  $\text{C}_1:\text{C}_3$  in the preparation of  $[\text{AsA}'_3]$ , as seen in Table 1.  $\text{AsCl}_3$  is a liquid at room temperature<sup>9</sup> and produces a relatively low  $\text{C}_1:\text{C}_3$  ratio ( $<3.7:1$ ) for both mechanochemical and solutions reactions, similar to  $\text{AsI}_3$  in toluene solution. Milling with the layered  $\text{AsI}_3$  more than doubles the  $\text{C}_1:\text{C}_3$  ratio obtained from  $\text{AsCl}_3$  in the mixer mill. Reactions with  $\text{AsCl}_3$  strongly favor metathesis over the redox pathway, producing very little  $\{\text{A}'\}_2$  when compared to  $\text{AsI}_3$ . Although there are individual exceptions, the yields from  $\text{AsCl}_3$  under mechanochemical reactions are generally comparable, and often somewhat better, than those from solution. The original report of  $[\text{AsA}'_3]$ <sup>5</sup> found that it was formed in 80% yield from a 5 min grind in a planetary ball mill, but 64% from a solution reaction in hexanes. Table 1 expands on this, comparing yields of  $[\text{AsA}'_3]$  from a mixer mill reaction and solution. The yields from  $\text{AsCl}_3$  are marginally higher in solution than in a mixer mill, but as just noted, its liquid state brings its behavior closer to what would be expected from a solution reaction rather than one conducted under solvent-free conditions.

The structure of the two antimony halides,  $\text{SbCl}_3$  and  $\text{SbI}_3$ , are more similar than in the arsenic case, but significant distinctions remain between them. After examining differences through reactions in the planetary and mixer mills, pre-grinding experiments, and use of multiple jar materials, it is clear that compared to  $\text{SbCl}_3$ ,  $\text{SbI}_3$  yields  $[\text{SbA}'_3]$  with a higher  $\text{C}_1:\text{C}_3$  ratio, but also more  $\{\text{A}'\}_2$  and decreased yield. For example, a 60 min grind in the planetary mill in  $\text{ZrO}_2$  jars produced a  $\text{C}_1:\text{C}_3$  ratio of 3.8 and a 25% yield with  $\text{SbI}_3$ , but a 2.8  $\text{C}_1:\text{C}_3$  ratio and 60% yield with  $\text{SbCl}_3$ . The parallel layers of solid  $\text{SbI}_3$  resemble those of  $\text{AsI}_3$  more than the zig-zag layers of  $\text{SbCl}_3$ , evidently leading to a greater preference for the  $\text{C}_1$  form when  $\text{SbI}_3$  is used. As with the arsenic derivative, yields of  $[\text{SbA}'_3]$  are favored somewhat under mechanochemical conditions. As one example, using  $\text{SbCl}_3$  for a 10 min grind in  $\text{ZrO}_2$  jars in a planetary mill provides a 72% yield of  $[\text{SbA}'_3]$ ; a 3 h reaction in hexanes provides 48%.



**Table 1** Effect of arsenic precursor and reaction environment on  $[\text{AsA}'_3]$  diastereomer formation

Entry	As source	Reaction conditions <sup>a</sup>	Yield (%)	$\text{C}_1 : \text{C}_3$ ratio	$[\text{AsA}'_3] : \{\text{A}'\}_2$ ratio
1	$\text{AsCl}_3$	Toluene	80( $\pm 4$ )	3.65( $\pm 0.03$ )	14( $\pm 5$ )
2	$\text{AsCl}_3$	MM	70( $\pm 1$ )	3.19( $\pm 0.01$ )	14( $\pm 5$ )
3	$\text{AsI}_3$	Toluene	28( $\pm 8$ )	2.60( $\pm 0.09$ )	0.6( $\pm 0.2$ )
4	$\text{AsI}_3$	MM	44( $\pm 1$ )	6.7( $\pm 0.2$ )	1.4( $\pm 0.2$ )

<sup>a</sup> Toluene = 3 h reaction time, room temperature; MM (mixer mill) = 10 min, 30 Hz;  $2 \times 3.5$  g stainless steel ball bearings.

#### Variable 4: mechanochemical equipment specifics

**Mill type.** Consistent with the original report of  $[\text{EA}'_3]$  synthesis,<sup>5</sup> there is little to no change in the  $\text{C}_1 : \text{C}_3$  ratio for  $[\text{AsA}'_3]$  or  $[\text{SbA}'_3]$  over extended reaction times when reactions are conducted in a planetary mill, using either stainless steel or zirconia jars. However, when  $[\text{AsA}'_3]$  is prepared in a mixer mill, increased milling time led to a detectable decrease in  $\text{C}_1 : \text{C}_3$  with both stainless steel and Teflon jars (Table 2). The same was also true for reactions to form  $[\text{SbA}'_3]$  (Fig. S12†).

The trends in the  $[\text{EA}'_3] : \{\text{A}'\}_2$  ratio and yield for  $[\text{AsA}'_3]$  follow the same trend as  $\text{C}_1 : \text{C}_3$  (Fig. S1–S3†). For  $[\text{SbA}'_3]$ , the  $[\text{SbA}'_3] : \{\text{A}'\}_2$  ratio decreased at longer reaction times under all conditions, but the rate of decrease was greatest for mixer mill reactions (Fig. S13 and S14†). The yields of  $[\text{AsA}'_3]$  and  $[\text{SbA}'_3]$  were consistent over time when using the planetary mill, but yields decreased at longer reaction times in the mixer mill.

**Ball and jar material.** Stainless steel balls can cause reduction during reactions,<sup>10</sup> but their widespread use persists due to their lower cost and higher durability than other milling options. Jar materials<sup>11</sup> and mill type<sup>12</sup> are also known to affect mechanochemical outcomes, underscoring the fact that their identity is not a variable that can be routinely discounted. Tests were made with planetary jars made of zirconia and stainless steel and with mixer mill jars of Teflon and stainless steel. For all reactions, the milling jar and balls were made of the same material (except that reactions conducted in Teflon jars used  $\text{ZrO}_2$  balls).

The highest  $\text{C}_1 : \text{C}_3$  ratio  $[\text{AsA}'_3]$  was found from short reaction times using Teflon mixer mill jars (Table 2, entries 1 and 2), notably higher (>30%) than comparable reactions using stainless steel (entries 3 and 4) (With a short grinding time of 5 min,

the Teflon/MM environment yielded a  $\text{C}_1 : \text{C}_3$  ratio of 11.1, the highest  $\text{C}_1$  enrichment we have yet observed; it is 37% higher than the 8.1 ratio found with stainless steel/MM). In the planetary mill, reactions in zirconia jars (entries 5 and 6) yielded a lower  $\text{C}_1 : \text{C}_3$  ratio than in stainless steel (7 and 8).

The highest  $\text{C}_1 : \text{C}_3$  ratio for  $[\text{SbA}'_3]$  was observed using antimony iodide and stainless-steel planetary jars at short reaction times or using zirconia planetary jars at long reaction times. In general, however, the  $\text{C}_1 : \text{C}_3$  ratio does not appear to be significantly dependent on the jar material for  $[\text{SbA}'_3]$  (Fig. S12†).

Generally, the  $[\text{EA}'_3]$  yield and the  $[\text{EA}'_3] : \{\text{A}'\}_2$  ratio is the lowest using stainless steel materials, owing to higher rates of redox activity, an effect similar to that previously observed in other mechanochemical syntheses.<sup>10,13</sup> The effects were greater for the metal iodides than antimony chloride. Across the reactions, yields and the  $[\text{EA}'_3] : \{\text{A}'\}_2$  ratio decreased with increasing reaction time (Fig. S2, S3, S13 and S14†).

**Ball size.** Ball size was not controlled when comparing the mixer mill (large balls) and planetary mill (small balls), so several reactions in the mixer mill were performed in stainless steel jars to prepare  $[\text{AsA}'_3]$ . For each reaction, a total of 7 g of stainless-steel balls were used (2 large balls or 14 small balls). The change in the  $\text{C}_1 : \text{C}_3$  ratio is not statistically significant with the smaller balls; with the larger balls the decline was noticeable (Fig. 7). The smaller balls consistently give higher  $\text{C}_1 : \text{C}_3$  ratio than the larger balls.

The yield and the  $[\text{AsA}'_3] : \{\text{A}'\}_2$  ratio were both higher for the small ball bearings than the large, and all saw a decrease as reaction times increased (Fig. S4 and S5†).

**Decomposition studies.** As the reaction of  $\text{AsI}_3$  and  $\text{KA}'$  is rapid (up to quantitative yield in 5 min) and the yield generally

**Table 2** Effect of the milling environment on the  $\text{C}_1 : \text{C}_3$  ratio of  $[\text{AsA}'_3]$ <sup>a</sup>

Entry	Milling environment	Time (min)	$\text{C}_1 : \text{C}_3$ ratio
1	Teflon, MM	10	10.7( $\pm 0.4$ )
2	Teflon, MM	60	8.5( $\pm 0.1$ )
3	Stainless, MM	10	6.7( $\pm 0.2$ )
4	Stainless, MM	60	6.0( $\pm 0.5$ )
5	$\text{ZrO}_2$ , PM	10	6.46( $\pm 0.01$ )
6	$\text{ZrO}_2$ , PM	60	6.7( $\pm 0.4$ )
7	Stainless, PM	10	7.7( $\pm 0.8$ )
8	Stainless, PM	60	8.5( $\pm 1.0$ )

<sup>a</sup> MM = mixer mill; PM = planetary mill.

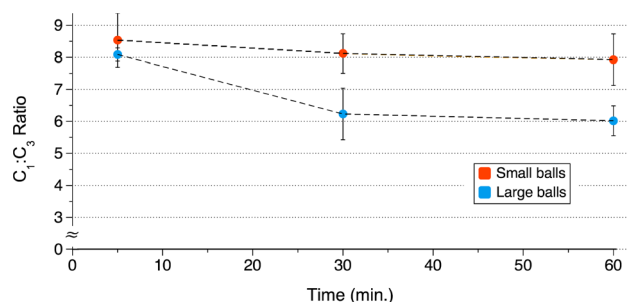


**Fig. 7** Effect of ball size on the  $\text{C}_1 : \text{C}_3$  ratio of  $[\text{AsA}'_3]$  (small ball = 4.8 mm, 0.5 g per ball; large ball = 9.5 mm, 3.5 g per ball).



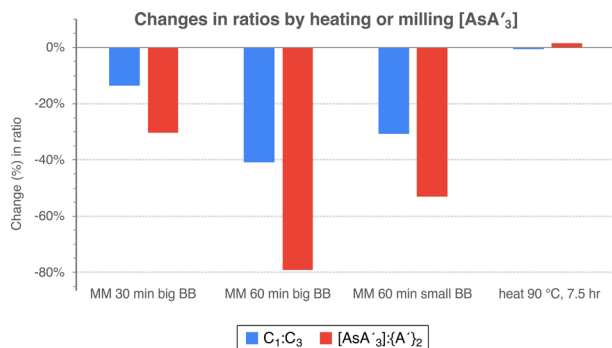


Fig. 8 Effect of grinding prepared [AsA'3] with either large (9.5 mm) or small (4.8 mm) stainless steel ball bearings. The negligible effect of heating in solution is also evident.

decreases with increased milling time, decomposition studies were performed in which [AsA'3] was milled alone or with 3 equiv. of potassium iodide (*i.e.*, a reaction by-product) in a mixer mill for 30–60 min. The change in C<sub>1</sub>:C<sub>3</sub> ratio (Fig. S10†) and [AsA'3]:{A'}<sub>2</sub> ratio (Fig. S11†) before and after milling were monitored. There is little difference in either ratio when KI is present or absent, so it appears that KI does not play a significant role in the decomposition of [AsA'3], the formation of {A'}<sub>2</sub>, or in changing the C<sub>1</sub>:C<sub>3</sub> ratio.

As the presence of KI does not affect decomposition, the data in Fig. 8 omits experiments where KI was added (Table S6†). In this case, the percent change of the C<sub>1</sub>:C<sub>3</sub> ratio (blue) or [AsA'3]:{A'}<sub>2</sub> ratio (red) is shown both before and after milling/heating. The change from heating is negligible, which is consistent with the original report of the synthesis.<sup>5</sup> All milling experiments saw a decrease in C<sub>1</sub>:C<sub>3</sub> and a decrease of [AsA'3] relative to {A'}<sub>2</sub>. The percent change in [AsA'3]:{A'}<sub>2</sub> is about twice that of C<sub>1</sub>:C<sub>3</sub>. Consistent with other findings, increased time and larger balls lead to more decomposition and less formation of the C<sub>1</sub> diastereomer.

Examining only diastereomeric ratios alone leaves unanswered the question of whether more of the C<sub>3</sub> diastereomer is produced with increased milling time or whether less of the C<sub>1</sub> form is produced. That the latter is more important is indicated by the masses of the products in some representative reactions to form [AsA'3] (Table 3). For both small and large balls, the amounts of both diastereomers decreases, but less of the C<sub>1</sub> form is isolated relative to the more symmetric C<sub>3</sub>. As discussed below, it is possible that the solid C<sub>1</sub> form is degraded more rapidly than the oily/liquid C<sub>3</sub>.

## Discussion

The heavy Group 15 [EA'3] complexes constitute a well-defined system in which two diastereomers are formed for each element, and whose ratio is affected by the anisotropic environment in which they are formed. Our working hypothesis has been that the extent to which that environment is maintained or modified during synthesis will affect the diastereomeric ratio. The question is then to determine how mechanochemical variables affect that ratio.

### Reproducibility

An issue that was critical to this research was that of reproducibility.<sup>14</sup> The reactions under each set of conditions were run at least twice, more (3 or 4 times) when the two data points displayed more than a 50% difference in the C<sub>1</sub>:C<sub>3</sub> or [EA'3]:{A'}<sub>2</sub> ratios. Solid-state reactions are inherently heterogeneous; a major benefit of solution-phase reactions is the creation of homogeneous mixtures. The problem of mixing is exacerbated when running reactions on a small scale. Furthermore, the chosen metal halides were used in their crystalline form and not as powders. As such, even though there was an attempt to minimize this as much as possible, there was heterogeneity in starting particle size. Across our studies, the ratio of C<sub>1</sub>:C<sub>3</sub> was more consistent across multiple experiments under the same conditions, whereas the [EA'3]:{A'}<sub>2</sub> ratio and yield were more varied.

### Variable 1: LAG

The precise function of the solvent in LAG reactions is still under debate. In some cases, the liquid appears to interact only physically, functioning primarily as a lubricant and promoting molecular diffusion.<sup>15</sup> The use of LAG solvent has been described as 'catalytic', as substoichiometric amounts of liquid can increase reaction rates.<sup>16</sup> The role of solvents in this range can be multifaceted and in some cases even inhibitory.<sup>17</sup>

In this system, it seems that the solubility of the intermediates of product formation may play a substantial role modifying the C<sub>1</sub>:C<sub>3</sub> ratio. Crystalline AsI<sub>3</sub> is slightly soluble in hexanes, and insoluble in HMDSO, but their use in LAG equally affects the C<sub>1</sub>:C<sub>3</sub> ratio. In contrast, the product [AsA'3] is highly soluble in either solvent. While not experimentally testable (as these species are not isolable), the proposed intermediates of metathesis, [AsA'I<sub>2</sub>] and [AsA'2I], would each be more soluble in the LAG liquid than AsI<sub>3</sub>, with solubility increasing with each substitution with an allyl. Hence in the presence of hexanes/

Table 3 Effect of the milling time on the C<sub>1</sub>:C<sub>3</sub> composition of [AsA'3]<sup>a</sup>

Ball size	Time (min)	C <sub>1</sub> :C <sub>3</sub> ratio	Mass C <sub>1</sub>	Mass C <sub>3</sub>	[AsA'3]:{A'} <sub>2</sub>	Mass {A'} <sub>2</sub>
Small	5	8.5	89.5	10.5	12.5	8
Small	60	7.9	64.8	8.2	5.6	13
Large	5	8.1	77.4	9.6	5.4	16
Large	60	6.0	36	6	1.2	35

<sup>a</sup> Small ball = 4.8 mm, 0.5 g per ball; large ball = 9.5 mm, 3.5 g per ball. Masses are in mg.



HMDSO, the metathesis intermediate  $[\text{AsA}'\text{I}_2]$  should be more soluble in hexanes and could diffuse away from the  $\text{AsI}_3$  lattice (and the anisotropic environment) before additional substitution occurs, producing less  $\text{C}_1$  and relatively more of the  $\text{C}_3$  diastereomer. The more solvent present in the system, the more diffusion/detachment can proceed. It should be noted that although the experiments were conducted well within the standard LAG region ( $\eta < 1$ ), the  $\eta$  value only takes into account the mass and volume of solvent.<sup>6</sup> On a molecular level, three or more molecules of the LAG solvent were present for every metal center, providing enough for molecular diffusion to occur.<sup>18</sup> Although a structure-directing effect has been observed before with LAG in the formation of host–guest complexes, co-crystals, and polymorphs,<sup>19</sup> in which liquid polarity, the  $\eta$  value, and interactions between the liquid and the reactants have been implicated, it is rare to observe the effect displayed by the  $[\text{EA}'_3]$  complexes, in which LAG affects organometallic reaction intermediates.<sup>4a</sup>

### Variable 2: pre-grinding

Any effect of pre-grinding  $\text{AsI}_3$  on the  $\text{C}_1 : \text{C}_3$  ratio in the mixer mill evidently happens within the first few minutes, as there is no apparent change when grinding from 5–30 min. Grinding in the planetary mill for up to 45 min shows a modest decrease, which might be related to the greater shearing forces in a planetary mill.<sup>20</sup> Such forces can induce lattice defects, such as vacancies, dislocations, stacking faults, and grain boundaries, and cause partial reordering of the crystalline lattice.<sup>21</sup> These disruptions could serve to degrade the environment on the surface of  $\text{AsI}_3$  particles. The effect is muted with the antimony precursors, but the  $\text{C}_1 : \text{C}_3$  ratio is smaller than that with the arsenic counterparts to begin with, so there is less room for change.

### Variable 3: elemental precursor

Examination of the metal precursors ( $\text{AsCl}_3$  vs.  $\text{AsI}_3$ , or  $\text{SbCl}_3$  vs.  $\text{SbI}_3$ ) reinforces the interpretation that the solid-state lattice of the precursor affects the stereochemical outcome of the reaction. In addition, iodide salts see an increase in redox activities (more  $\{\text{A}'\}_2$ ) versus chloride salts, due to weaker E–I bonds and the increased stability of the iodide radical.<sup>22</sup> Furthermore, in the presence of iodine ( $\text{I}_2$ ), allyl complexes of s-block and transition metals promote allyl coupling.<sup>23</sup> For both arsenic and antimony, there is a trade-off between stereoselectivity and chemoselectivity (higher  $\text{C}_1 : \text{C}_3$  ratios are associated with lower  $[\text{EA}'_3] : \{\text{A}'\}_2$  ratios).

### Variable 4: mechanochemical equipment specifics

The trends in  $\text{C}_1 : \text{C}_3$  with jar milling material (*i.e.*, reactions in zirconia jars yielded a lower  $\text{C}_1 : \text{C}_3$  ratio than stainless steel, and Teflon provided the highest of all (Table 2)) suggest that a softer jar material favors an increase of  $\text{C}_1$ , while a harder material favors a relative increase of  $\text{C}_3$  (zirconia has a Mohs hardness of 8.0–8.5, stainless steel is *ca.* 6.5, and Teflon from 2.0–2.5).<sup>24</sup> This appears to be more important than the density,

as steel (density  $\approx 7.5 \text{ g mL}^{-1}$ ) is denser than zirconia ( $\approx 5.6 \text{ g mL}^{-1}$ ).

Another possible contributor to the lower  $\text{C}_1 : \text{C}_3$  ratio with harder grinding media may be related to deformations that occur to the reagents under pressure. For example, in the layers of arsenic triiodide are identifiable  $\text{AsI}_3$  units. The iodine anions are arranged in an hexagonal close packed (hcp) lattice with arsenic cations filling two-thirds of the octahedral holes in every other layer (Fig. 2b).<sup>25</sup> Each arsenic is covalently bonded to three iodine atoms (2.65 Å), with another set of three iodine atoms further away (3.62 Å) but within the sum of van der Waals radii (*ca.* 3.9 Å).<sup>26</sup> Under high pressure ( $>1.7 \text{ GPa}$ ), it has been found that  $\text{AsI}_3$  undergoes a phase transformation from the anisotropic phase to a more centrosymmetric phase.<sup>27</sup> The intermolecular separation of  $\text{AsI}_3$  units decreases, new bonds form, and the environment around arsenic becomes similar to that of bismuth in hcp  $\text{BiI}_3$ .<sup>28</sup> When the metal center is in this more symmetric (*i.e.*, more solution-like) environment at the moment of impact, the  $\text{C}_3$  isomer would presumably form faster than when the metal center is in the more anisotropic form at atmospheric pressure.

That this is not an unrealistic scenario reflects the fact that in ball milling experiments the impacts between balls or a between ball and the jar create a small area of high pressure on the powder trapped within the collision; this pressure can be on the order of gigapascals (Maurice and Courtney reported 2–4 GPa in their experiments).<sup>29</sup> Additionally, ball milling has been shown to induce phase transformations in particles at lower temperatures<sup>30</sup> or pressures<sup>31</sup> than reported for bulk materials. The high level of shear forces and structural defects that occur in ball milling experiments lead to these depressed transition conditions.<sup>31a</sup> A related phase transformation under pressure has been reported for  $\text{SbI}_3$  ( $>1.4 \text{ GPa}$ ).<sup>32</sup>

In the formation of  $[\text{AsA}'_3]$ , small grinding balls regularly give higher  $\text{C}_1 : \text{C}_3$  ratios than the larger balls. This trend is consistent with that of the jar material, in that lower energy collisions (with smaller balls) lead to more of the  $\text{C}_1$  diastereomer than  $\text{C}_3$ . Emmerling and coworkers have found a linear correlation between the mass of a single ball and the reaction rate, even when the total mass of the balls is the same.<sup>4c</sup> Our data are consistent with this trend.<sup>33</sup>

### Variable 5: decomposition studies

The route of decomposition of  $[\text{EA}'_3]$  complexes is not currently known, although since  $\{\text{A}'\}_2$  is a major decomposition product, it is likely that the compounds undergo homolytic E–C bond cleavage to form  $\cdot\text{A}'$  radicals, which couple to form  $\{\text{A}'\}_2$ . Similar decomposition does not occur in solution at temperatures up to 90 °C, a thermal environment comparable to the energetics reached in a mixer mill (Fig. 8).<sup>34</sup> Hence it appears that this is a mechanochemically specific mode of decomposition, perhaps driven by transient build-up and relaxation of strain.<sup>35</sup> The fact that the  $\text{C}_1 : \text{C}_3$  ratio decreases during decomposition suggests that the  $\text{C}_1$  form is decomposing more quickly than the more symmetric  $\text{C}_3$  diastereomer. Although this point is not certain, the fact that the  $\text{C}_1$  forms of both  $[\text{AsA}'_3]$  and  $[\text{SbA}'_3]$  are



crystalline solids at room temperature, whereas the C<sub>3</sub> isomer of [SbA<sub>3</sub><sup>+</sup>] is a liquid at room temperature and that for [AsA<sub>3</sub><sup>+</sup>] is a near-liquid/oil<sup>5</sup> may mean that the C<sub>3</sub> conformations are not subject to the same levels of compressive stress that the more rigid C<sub>1</sub> forms are.

## Conclusions

A unique variable in mechanosynthesis is the possibility of employing anisotropic solids as reagents that have the ability to direct outcomes in ways that are different from those in solution. The diastereomeric pairs of Group 15 allyl complexes examined here also indicate the multiple ways this can be manipulated, from the use of LAG to the material of the grinding jar. In general, anything that degrades the lattice (use of a mixer mill or larger balls) or removes the incipient product from the anisotropic environment (LAG is especially important) can shift the diastereomeric ratio closer to the ratios found in solution. The Group 15 allyls represent a specific model system, but it is possible that some of these findings will find counterparts in mechanochemical syntheses with other anisotropic reagents.

In addition to the use of layered solids, anisotropy could potentially be introduced into mechanochemical environments in other ways, such as with solid additives or liquid crystals in LAG.<sup>36</sup> We are continuing to explore these possibilities.

## Conflicts of interest

There are no conflicts to declare.

## Acknowledgements

Financial support by the National Science Foundation (CHE-2155144) is gratefully acknowledged. Henry DeGroot is thanked for helpful discussions of data trends, and both he and Sonja Moons provided assistance in early exploratory reactions for this project. Dillon Button-Jennings is thanked for assisting in exploratory reactions and collecting SEM images. William Lowry is acknowledged for assistance with SEM sample preparation. We thank Jeremy Espano for collection of powder XRD data.

## Notes and references

- (a) L. Takacs, *JOM*, 2000, **52**, 12–13; (b) L. Takacs, *Chem. Soc. Rev.*, 2013, **42**, 7649–7659.
- S. Pagola, *Crystals*, 2023, **13**, 124.
- (a) J. Andersen and J. Mack, *Green Chem.*, 2018, **20**, 1435–1443; (b) J. M. Andersen and J. Mack, *Chem. Sci.*, 2017, **8**, 5447–5453; (c) L. E. Wenger and T. P. Hanusa, *Chem. Commun.*, 2023, **59**, 14210–14222.
- (a) T. Stolar, L. Batzdorf, S. Lukin, D. Žilić, C. Motillo, T. Friščić, F. Emmerling, I. Halasz and K. Užarević, *Inorg. Chem.*, 2017, **56**, 6599–6608; (b) H. Kulla, F. Fischer, S. Benemann, K. Rademann and F. Emmerling, *CrystEngComm*, 2017, **19**, 3902–3907; (c) F. Fischer, N. Fendel, S. Greiser, K. Rademann and F. Emmerling, *Org. Process Res. Dev.*, 2017, **21**, 655–659; (d) S. Mateti, M. Mathesh, Z. Liu, T. Tao, T. Ramireddy, A. M. Glushenkov, W. Yang and Y. I. Chen, *Chem. Commun.*, 2021, **57**, 1080–1092.
- N. R. Rightmire, D. L. Bruns, T. P. Hanusa and W. W. Brennessel, *Organometallics*, 2016, **35**, 1698–1706.
- T. Friščić, C. Mottillo and H. M. Titi, *Angew. Chem., Int. Ed.*, 2020, **59**, 1018–1029.
- S. Tanaka, M. Konishi, H. Imoto, Y. Nakamura, M. Ishida, H. Furuta and K. Naka, *Inorg. Chem.*, 2020, **59**, 9587–9593.
- K. T. Quisenberry, C. K. Gren, R. E. White, T. P. Hanusa and W. W. Brennessel, *Organometallics*, 2007, **26**, 4354–4356.
- J. Galy, R. Enjalbert, P. Lecante and A. Burian, *Inorg. Chem.*, 2002, **41**, 693–698.
- M. J. Rak, N. K. Saade, T. Friščić and A. Moores, *Green Chem.*, 2014, **16**, 86–89.
- L. Chen, M. O. Bovee, B. E. Lemma, K. S. M. Keithley, S. L. Pilson, M. G. Coleman and J. Mack, *Angew. Chem., Int. Ed.*, 2015, **54**, 11084–11087.
- S. R. Chauruka, A. Hassanpour, R. Brydson, K. J. Roberts, M. Ghadiri and H. Stitt, *Chem. Eng. Sci.*, 2015, **134**, 774–783.
- T. Auvray and T. Friščić, *Molecules*, 2023, **28**, 897.
- (a) A. M. Belenguer, G. I. Lampronti and J. K. M. Sanders, *JoVE*, 2018, e56824, DOI: [10.3791/56824](https://doi.org/10.3791/56824); (b) A. A. L. Michalchuk and F. Emmerling, *Angew. Chem., Int. Ed.*, 2022, **61**, e202117270; (c) J.-L. Do and T. Friščić, *ACS Cent. Sci.*, 2017, **3**, 13–19.
- M. Rodrigues, B. Baptista, J. A. Lopes and M. C. Sarraguça, *Int. J. Pharm.*, 2018, **547**, 404–420.
- (a) T. Friščić, *J. Mater. Chem.*, 2010, **20**, 7599–7605; (b) M. Tireli, M. Juribašić Kulcsár, N. Cindro, D. Gracin, N. Biliškov, M. Borovina, M. Ćurić, I. Halasz and K. Užarević, *Chem. Commun.*, 2015, **51**, 8058–8061.
- (a) M. Arhangelskis, D.-K. Bučar, S. Bordignon, M. R. Chierotti, S. A. Stratford, D. Voinovich, W. Jones and D. Hasa, *Chem. Sci.*, 2021, **12**, 3264–3269; (b) I. Brekalo, V. Martinez, B. Karadeniz, P. Orešković, D. Drapanauskaitė, H. Vriesema, R. Stenekes, M. Etter, I. Dejanović, J. Baltrusaitis and K. Užarević, *ACS Sustainable Chem. Eng.*, 2022, **10**, 6743–6754.
- R. J. Allenbaugh and A. Shaw, *Results Chem.*, 2023, **5**, 100827.
- (a) T. Friščić, A. V. Trask, W. D. S. Motherwell and W. Jones, *Cryst. Growth Des.*, 2008, **8**, 1605–1609; (b) F. Fischer, G. Scholz, S. Benemann, K. Rademann and F. Emmerling, *CrystEngComm*, 2014, **16**, 8272–8278; (c) D. Hasa, E. Miniussi and W. Jones, *Cryst. Growth Des.*, 2016, **16**, 4582–4588.
- X. Zhang, X. Liu, J. Zhao, W. Sun, Y. Zhang, J. Qiao, G. Xing and X. Wang, *Sustainability*, 2023, **15**, 1353.
- C. Suryanarayana, *Prog. Mater. Sci.*, 2001, **46**, 1–184.
- J. E. Huheey, E. A. Keiter and R. L. Keiter, *Inorg. Chem.: Principles of Structure and Reactivity*, Harper Collins, New York, 4th edn, 1993.
- (a) K. T. Quisenberry, R. E. White, T. P. Hanusa and W. W. Brennessel, *New J. Chem.*, 2010, **34**, 1579–1584; (b) R. Baker, *Chem. Rev.*, 1973, **73**, 487–530; (c) K. E. Torraca





- and L. McElwee-White, *Coord. Chem. Rev.*, 2000, **206–207**, 469–491; (d) P. Jochmann, T. S. Dols, T. P. Spaniol, L. Perrin, L. Maron and J. Okuda, *Angew. Chem., Int. Ed.*, 2009, **48**, 5715–5719.
- 24 M. J. Frost, in *Mineralogy*, Springer US, Boston, MA, 1983, pp. 283–284, DOI: [10.1007/0-387-30720-6\\_84](https://doi.org/10.1007/0-387-30720-6_84).
- 25 R. Enjalbert and J. Galy, *Acta Crystallogr., Sect. B: Struct. Crystallogr. Cryst. Chem.*, 1980, **36**, 914–916.
- 26 S. Alvarez, *Dalton Trans.*, 2013, **42**, 8617–8636.
- 27 (a) A. Anderson, S. K. Sharma and Z. Wang, *High Pressure Res.*, 1996, **15**, 43–50; (b) H. C. Hsueh, R. K. Chen, H. Vass, S. J. Clark, G. J. Ackland, W. C. K. Poon and J. Crain, *Phys. Rev. B*, 1998, **58**, 14812–14822; (c) A. Saitoh, T. Komatsu and T. Karasawa, *Phys. Status Solidi B*, 2000, **221**, 573–581.
- 28 J. Trotter and T. Zobel, *Z. Kristallogr.*, 1966, **123**, 67–72.
- 29 D. R. Maurice and T. H. Courtney, *Metall. Trans. A*, 1990, **21**, 289–303.
- 30 (a) K. Linberg, B. Röder, D. Al-Sabbagh, F. Emmerling and A. A. L. Michalchuk, *Faraday Discuss.*, 2023, **241**, 178–193; (b) A. P. Amrute, Z. Łodziana, H. Schreyer, C. Weidenthaler and F. Schüth, *Science*, 2019, **366**, 485–489; (c) P. N. Kuznetsov, L. I. Kuznetsova, A. M. Zhyzhaev, V. I. Kovalchuk, A. L. Sannikov and V. V. Boldyrev, *Appl. Catal., A*, 2006, **298**, 254–260; (d) I. J. Lin and S. Nadiv, *Mater. Sci. Eng.*, 1979, **39**, 193–209.
- 31 (a) L. L. Driscoll, E. H. Driscoll, B. Dong, F. N. Sayed, J. N. Wilson, C. A. O'Keefe, D. J. Gardner, C. P. Grey, P. K. Allan, A. A. L. Michalchuk and P. R. Slater, *Energy Environ. Sci.*, 2023, **16**, 5196–5209; (b) E. E. McBride, A. Krygier, A. Ehnes, E. Galtier, M. Harmand, Z. Konôpková, H. J. Lee, H. P. Liermann, B. Nagler, A. Pelka, M. Rödel, A. Schropp, R. F. Smith, C. Spindloe, D. Swift, F. Tavella, S. Toleikis, T. Tschentscher, J. S. Wark and A. Higginbotham, *Nat. Phys.*, 2019, **15**, 89–94.
- 32 H. Kurisu, T. Tanaka, T. Karasawa and T. Komatsu, *Jpn. J. Appl. Phys.*, 1993, **32**, 285.
- 33 S. S. Razavi-Tousi and J. A. Szpunar, *Powder Technol.*, 2015, **284**, 149–158.
- 34 (a) L. Takacs and J. S. McHenry, *J. Mater. Sci.*, 2006, **41**, 5246–5249; (b) K. S. McKissic, J. T. Caruso, R. G. Blair and J. Mack, *Green Chem.*, 2014, **16**, 1628–1632; (c) R. Schmidt, H. Martin Scholze and A. Stolle, *Int. J. Ind. Chem.*, 2016, **7**, 181–186.
- 35 R. T. O'Neill and R. Boulatov, *Nat. Rev. Chem.*, 2021, **5**, 148–167.
- 36 (a) C. M. Gordon, J. D. Holbrey, A. R. Kennedy and K. R. Seddon, *J. Mater. Chem.*, 1998, **8**, 2627–2636; (b) I. J. B. Lin and C. S. Vasam, *J. Organomet. Chem.*, 2005, **690**, 3498–3512.

